Homogeneous freezing of water starts in the subsurface

Luboš Vrbka and Pavel Jungwirth

Institute of Organic Chemistry and Biochemistry, Academy of Sciences of the Czech Republic, and Center for Complex Molecular Systems and Biomolecules, Flemingovo nám. 2, 16610 Prague 6, Czech Republic

Abstract

Molecular dynamics simulations of homogeneous ice nucleation in extended aqueous slabs show that freezing preferentially starts in the subsurface. The top surface layer remains disordered during the freezing process. The subsurface accommodates better than the bulk the increase of volume connected with freezing. It also experiences strong electric fields caused by oriented surface water molecules, which can enhance ice nucleation. Our computational results shed new light on the experimental controversy concerning the bulk vs surface origin of homogeneous ice nucleation in water droplets. This has important atmospheric implications for the microphysics of formation of high altitude clouds.

Introduction

In most cases, water in nature freezes heterogeneously, i.e., in contact with pieces of ice or minerals at moderately sub-zero (Celsius) temperatures. However, without a contact with such pre-existing nuclei water droplets can be supercooled below -30 ^{o}C before homogeneous freezing occurs.[1] Homogeneous freezing was shown to be crucial for the microphysics of formation of high altitude cirrus clouds and polar stratospheric clouds, as well as for glaciation of thunderclouds.[2-5] There is an ongoing discussion whether homogeneous ice nucleation starts in the aqueous bulk or at the surface of the droplets. In the latter case, the freezing rate should strongly depend on the droplet size and surface contamination, which has important atmospheric consequences. However, the present experimental evidence is conflicting which opens the possibility for addressing the problem via molecular simulations. Homogeneous freezing in the aqueous bulk has been successfully simulated recently.[6] Here, we present molecular dynamics simulations of homogeneous freezing in aqueous slabs of varying sizes, where both bulk and surface ice nucleation can occur. The simulation results show with all molecular detail that homogeneous ice nucleation preferentially starts in the subsurface. The immediate surface with undercoordinated water molecules remains disordered during the whole process. The subsurface, which can better than the bulk accommodate the volume change during the onset of freezing and which is subject to a strong electric field due to oriented surface water molecules, turns out to be the ideal place for a spontaneous creation and growth of the ice nucleus. The present computational results help to resolve a persisting controversy concerning the spatial origin of homogeneous ice nucleation in water droplets, which has atmospheric implications for cloud microphysics and, consequently, for effects of pollution on the Earth's global radiative balance.

Based on thermodynamic arguments and analysis of experimental ice freezing rates it has been suggested recently that homogeneous freezing of aqueous droplets starts at the surface rather than in the bulk.[1,7,8] If true, this fact can have far reaching

atmospheric consequences. Homogeneous ice nucleation is prevalent in cirrus, polar stratospheric, and thunderstorm clouds.[2-5] Anthropogenic emissions of organic compounds and molecular nitric acid are deposited on cloud droplets and vary their interfacial properties. Should surface nucleation be important then human activity can influence the freezing rates of cloud droplets with important implications for atmospheric composition and the radiative balance of the Earth.[1] However, the evidence for homogeneous surface ice nucleation is conflicting. On one hand, higher freezing temperatures and faster freezing rates were observed for droplets with an ice-forming nucleus placed close to the surface compared to a bulk location.[9] On the other hand, recent laboratory measurements indicate that homogeneous ice freezing is a volume-proportional process with surface nucleation being potentially important for small droplets with radii below 20 μm.[10] In summary, it has been concluded that, based on existing thermodynamic nucleation models, as well as laboratory and atmospheric data, homogeneous ice nucleation at the surface can be neither confirmed nor disregarded.[11]

In this ambiguous situation, it has been suggested that molecular dynamics (MD) simulations could provide a fresh view on homogeneous nucleation at surfaces.[12] A recent computational study has indeed lent new insight into homogeneous nucleation in clusters of SF_6, showing that in this compound bulk nucleation dominates over the surface one.[13] In water, there have been numerous computational studies of heterogeneous freezing in contact with a patch of ice.[14-17] However, there is only a single successful MD study of homogeneous ice nucleation, where aqueous bulk was simulated and freezing was observed.[6] To the best of our knowledge, no attempts have been made so far to simulate homogeneous ice nucleation at the surface. Here, we report first MD simulations of homogeneous ice nucleation in systems containing both aqueous bulk and surface. A straightforward choice of such a system seems to be a water cluster. However, nanometer size clusters amenable to MD simulations have very different surface properties (curvature, surface

tension, etc.) than atmospheric droplets of micrometer to milimeter size. At the molecular level, the surface of the latter does not differ from an extended, flat surface.[5] Therefore, we have chosen to simulate homogeneous ice nucleation in extended aqueous slabs[18] with a bulk region in-between two parallel air/water interfaces.

Computational Details

MD simulations of homogeneous freezing of aqueous slabs were performed using a recently developed six-site interaction potential for water.[19] This potential was optimized for simulations of water and ice near the melting point and, unlike most other water models, exhibits a melting temperature very close to 0 ^{o}C (between 270 and 280 K).[19]

Simulated aqueous systems were placed in a rectangular prismatic box extended in the z-direction, and 3D periodic boundary conditions were applied. This resulted in the formation of infinite slabs with bulk region in-between two surfaces in the xy-plane. The smallest unit cells with approximate dimensions 13.5 x 15.5 x 100 Å^3 contained 192 water molecules. The original unit cell with dimensions of 13.5 x 15.5 x 29.5 Å^3 was chosen such as to correspond to a rectangular cell of ice Ih and, subsequently, the z-dimension was extended to 100 Å^3. Larger slabs were constructed by doubling or tripling the width of the original cell, yielding systems with 384 or 576 water molecules in the unit cell. The z-dimension was consequently prolonged to 180 or 270 Å, respectively.

As in the first MD study of homogeneous ice nucleation in aqueous bulk,[7] non-bonded interactions had to be cut off at a relatively short distance of 6.5 Å due to the small size of the simulation cells in the x- and y-dimensions. However, unlike in the previous simulations,[7] long range electrostatic interactions were accounted for using

the smooth particle mesh Ewald method, employing a pseudo-2D correction for the slab geometry.[20]

After preparation of the liquid water systems and adjusting the target temperature, the production runs followed. Newton equations of motion were propagated with a time step of 1 fs for 100 - 500 ns. The LINCS algorithm was used to constrain bonds involving hydrogen atoms.[21] Temperature was constrained using the Nose-Hoover thermostat.[22] The optimal freezing temperature and temperature coupling constant were determined in runs employing the smallest simulation cell. The results indicated that the fastest ice nucleation occurred at a temperature of 250 K maintained using a temperature coupling constant of 0.5 ps. For each of the three system sizes we carried out two simulations at the above temperature with different starting coordinates.

All calculations were performed using the GROMACS 3.3 program package[23] and took an equivalent of ~1000 CPU days on an Intel Xeon processor machine. Simulations were run in parallel, typically on 8 processors. Further increase of the number of processors was not effective due relatively small system sizes.

Results and Discussion

The main results of the MD simulations are visualized in Figures 1 and 2 which show series of snapshots from trajectories of the two larger systems (we do not present here snapshots of the smallest slab, where the results are similar but which has due to its limited size only a very small bulk region). Figure 1 depicts snapshots from two independent runs of the medium-sized slab. We only show the central unit cell, which contains 384 water molecules and which is periodically repeated to form an extended slab. The bulk region lies in-between the two surfaces, which are at the top and bottom of each snapshot. In both runs, an ice nucleus forms around 50 ns in the subsurface, as highlighted by the shaded regions. The slabs then almost completely

freeze within ~200 ns, leaving a thin quasi-liquid layer at each surface. Note that in the first trajectory another ice nucleus formed independently in the bottom subsurface around 110 ns. When the two freezing events spatially met a somewhat disordered contact zone was still left at 160 ns (fourth snapshot in Figure 1).

The situation is similar for the largest slab with 576 water molecules in the unit cell (Figure 2). Within the first trajectory a subsurface ice nucleus forms at around 150 ns and the whole system (except for the quasi-liquid surface layers) freezes within 500 ns. The second trajectory is more complex with two independent ice nuclei being formed simultaneously at around 230 ns in the subsurface and deeper in the bulk. Freezing then progresses fast from both nuclei, leaving eventually a narrow disordered contact zone which did not completely crystalize on the timescale of the present simulations (last snapshot in Figure 2).

In all investigated cases, homogeneous nucleation leads to formation of cubic ice Ic (Figures 1 and 2). This is a metastable form of the most common hexagonal ice Ih, with which it shares very similar physical properties (structure, density, heat capacity, etc.). Experimentally, cubic ice forms spontaneously during freezing of very small water droplets and thin ice films.[24] In particular, cubic rather than hexagonal ice was shown recently to be the dominant ice phase formed in polar stratospheric clouds.[25]

Present simulations show the preference for subsurface ice nucleation. To be fully quantitative, one should ideally perform hundreds or thousands of freezing trajectories in order to obtain a converged statistics of the spatial distribution of the nucleation events. Homogeneous ice nucleation is, however, a rare event, the description of which is at the current technical limits of MD simulations. As a matter of fact, only a single homogeneous ice nucleation trajectory has been reported so far, pertinent to bulk liquid.[6] Here, we report on six trajectories for slab systems of three

different sizes, possessing both bulk and surface regions, allowing us to follow with atomistic resolution ice nucleation events and to make semi-quantitative conclusions. In all cases, supercooling by about 30 K led eventually to homogenous freezing with ice nucleation always taking place in the subsurface (in one trajectory, an independent second ice nucleus developed deeper in the bulk).

The preferred ice nucleation in the subsurface has several physical reasons. The surface region can better accommodate the volume change connected with freezing than the aqueous bulk. However, the immediate surface of water is undercoordinated and disordered, and remains such even after freezing took place, forming a thin quasi-liquid surface layer.[26] Ice nucleation thus tends to start just below this layer, i.e., in the subsurface. Another physical reason can be the presence of a large electric field in the air/water interface due to preferential orientation of surface water molecules. A strong electric field was shown both computationally and experimentally to be a powerful ice nucleator.[27] Figure 3 shows the charge profile across a slab of liquid water, arising from partial charges on hydrogens and oxygens. While in the bulk region the overall charge vanishes on average due to random orientations of water molecules, at the two air/water interfaces there is a preferential water orientation resulting in a distinct non-monotonous charge profile. This is in accord with previous simulations and experiments, showing that such a charge profile results in a surface potential of neat water of the order of ~100 mV or larger.[28-20] Such a potential difference across the sub-nanometer wide interfacial region is equivalent to an electric field of $10^6 – 10^7$ V/cm, which is strong enough to positively influence ice nucleation.[27] Finally, water self-diffusion in the interfacial layer is slightly larger than that in the bulk region.[30] The higher water mobility can represent a kinetic advantage for ice nucleation in the subsurface compared to the bulk.

Atmospheric Implications

Homogeneous ice nucleation in the subsurface has important atmospheric implications. It has been suggested that enrichment of supercooled cloud droplets by organic surfactants will hamper the formation of an ice nucleus at the surface.[1] The subsurface, which we found to be the preferential site for ice nucleation, will also feel the effect of the adsorbed organic material, albeit to a lesser extent than the top surface layer. We thus conclude that anthropogenic emissions will have an effect on composition and physical state of high altitude clouds and, consequently, on radiative properties of these atmospheric particles, although this effect could be smaller than estimated assuming surface nucleation.

Acknowledgment

We thank Marcelo Carignano and Igal Szleifer for sharing their manuscript with us prior to publication and the *META*Centrum in Brno for generous allocation of computer time. Support from the Czech Ministry of Education (grants LC512 andME644) and via the NSF-funded Environmental Molecular Science Institute (grants CHE 0431312 and 0209719) is gratefully acknowledged. L. V. acknowledges support from the Granting Agency of the Czech Republic (grant 203/05/H001).

References

1. Tabazadeh, A.; Djikaev, Y. S.; Reiss, H. *Proc. Natl. Acad. Sci.* **2002**, *99*, 15873.
2. Heymsfield, A. J.; Miloshevich, L. M. *J. Atmos. Sci.* **1993**, *50*, 2335.
3. Rogers, D. C.; DeMott, P. J.; Kreidenweis, S.; Chen, Y. *Geophys. Res. Lett.* **1998**, *25*, 1383.
4. Chang, H. A.; Koop, T.; Molina, L. T.; Molina, M. J. *J. Phys. Chem. A* **1999**, *103*, 2673.
5. Prupacher, H.; Klett, J. D. *Microphysics of Clouds and Precipitation*, Kluwer Academic Publishers: Dordrecht, 1998.
6. Matsumoto, M.; Saito, S.; Ohmine, I. *Nature* **2002**, *416*, 409.
7. Tabazadeh, A.; Djikaev, Y. S.; Hamill, P.; Reis, H. *J. Phys. Chem. A* **2002**, *106*, 10238.
8. Tabazadeh, A. *Atmos. Chem. Phys.* **2003**, *3*, 863.
9. Shaw, R. A.; Durant, A. J.; Mi, Y. *J. Phys. Chem. B* **2005**, *109*, 9865.
10. Duft, D.; Leisner, T. *Atmos. Chem. Phys. Discuss.* **2004**, *4*, 3077.
11. Kay, J. E.; Tsemekhman, V.; Larson, B.; Baker, M.; Swanson, B. *Atmos. Chem. Phys. Discuss.* **2003**, *3*, 3361.
12. Sastry, S. *Nature* **2005**, *438*, 746.
13. Turner, G. W.; Bartell, L. S. *J. Phys. Chem. A* **2005**, *109*, 6877.
14. Nada, H.; van der Eerden, J. P.; Furukawa, Y. *J. Crystal Growth* **2004**, *266*, 297.
15. Bryk, T.; Haymet, A. D. J. *J. Chem. Phys.* **2002**, *117*, 10258.
16. Carignano, M. A.; Shepson, P. B.; Szleifer, I. *Mol. Phys.* **2005**, *103*, 2957.
17. Vrbka, L.; Jungwirth, P. *Phys. Rev. Lett.* 2005, *95*, 148501.
18. Wilson, M. A.; Pohorille, A. *J. Chem. Phys.* **1991**, *95*, 6005.

19. Nada, H.; van der Eerden, J. P. *J. Chem. Phys.* **2003**, *118*, 7401.

20. Yeh, I.-C.; Berkowitz, M. L. *J. Chem. Phys.* **1999**, *111*, 3155.

21. Hess, B.; Bekker, H.; Berendsen, H. J. C.; Fraaije, J. G. E. M. *J. Comp. Chem.* **1997**, *18*, 1463.

22. Nose, S. *Mol. Phys.* **1984**, *52*, 255.

23. Lindahl, E.; Hess, B.; van der Spoel, D. *J. Mol. Mod.* **2001**, *7*, 306.

24. Morishige, K.; Uematsu, H. *J. Chem. Phys.* **2005**, *122*, 044711.

25. Murray, B. J.; Knopf, D. A.; Bertram, A. K. *Nature* **2005**, *43*4, 202.

26. Furukawa, Y.; Nada, H. *J. Phys. Chem. B* **1997**, *101*, 6167.

27. Svishev, I. M.; Kusalik, P. G. *J. Am. Chem. Soc.* **1996**, *118*, 649.

28. Wilson, M. A.; Pohorille, A.; Pratt, L. R. *J. Chem. Phys.* **1988**, *88*, 3281.

29. Paluch, M. *Adv. Colloid Interface Sci.* **2000**, *84*, 27.

30. Taylor, R. S.; Dang, L. X.; Garrett, B. C. *J. Phys. Chem*. **1996**, *10*0, 11720.

Figure captions:

Fig. 1: Four snapshots from each of the two homogeneous freezing trajectories of the medium-sized slab. Only the unit cell, containing 384 water molecules, is depicted. Periodic repetition of the unit cell along the axes defining the two shorter dimensions of the cell results in an extended slab with a bulk region in-between two surfaces (at the top and bottom of the snapshots). The shaded regions highlight the subsurface ice nuclei, spontaneously formed at ~50 ns (both trajectories) and around 110 ns (first trajectory).

Fig. 2: Four snapshots from each of the two homogeneous freezing trajectories of the large slab. Only the unit cell, containing 576 water molecules, is depicted. Periodic repetition of the unit cell along the axes defining the two shorter dimensions of the cell results in an extended slab with a bulk region in-between two surfaces (at the top and bottom of the snapshots). The shaded regions highlight the ice nucleus, spontaneously formed in the subsurface at ~150 ns (first trajectory) or the two ice nuclei (one in the subsurface and one deeper in the bulk) simultaneous formed at around 230 ns (second trajectory).

Fig. 3: Charge distribution across the smallest water slab prior to freezing. Note the distinct non-monotoneous charge profiles in the surface regions (around -15 and 15 Å). Charge in the bulk region vanishes on average with fluctuations due to finite system size and averaging over a short period. Water density across the slab is also depicted.

Fig. 1 (Vrbka & Jungwirth)

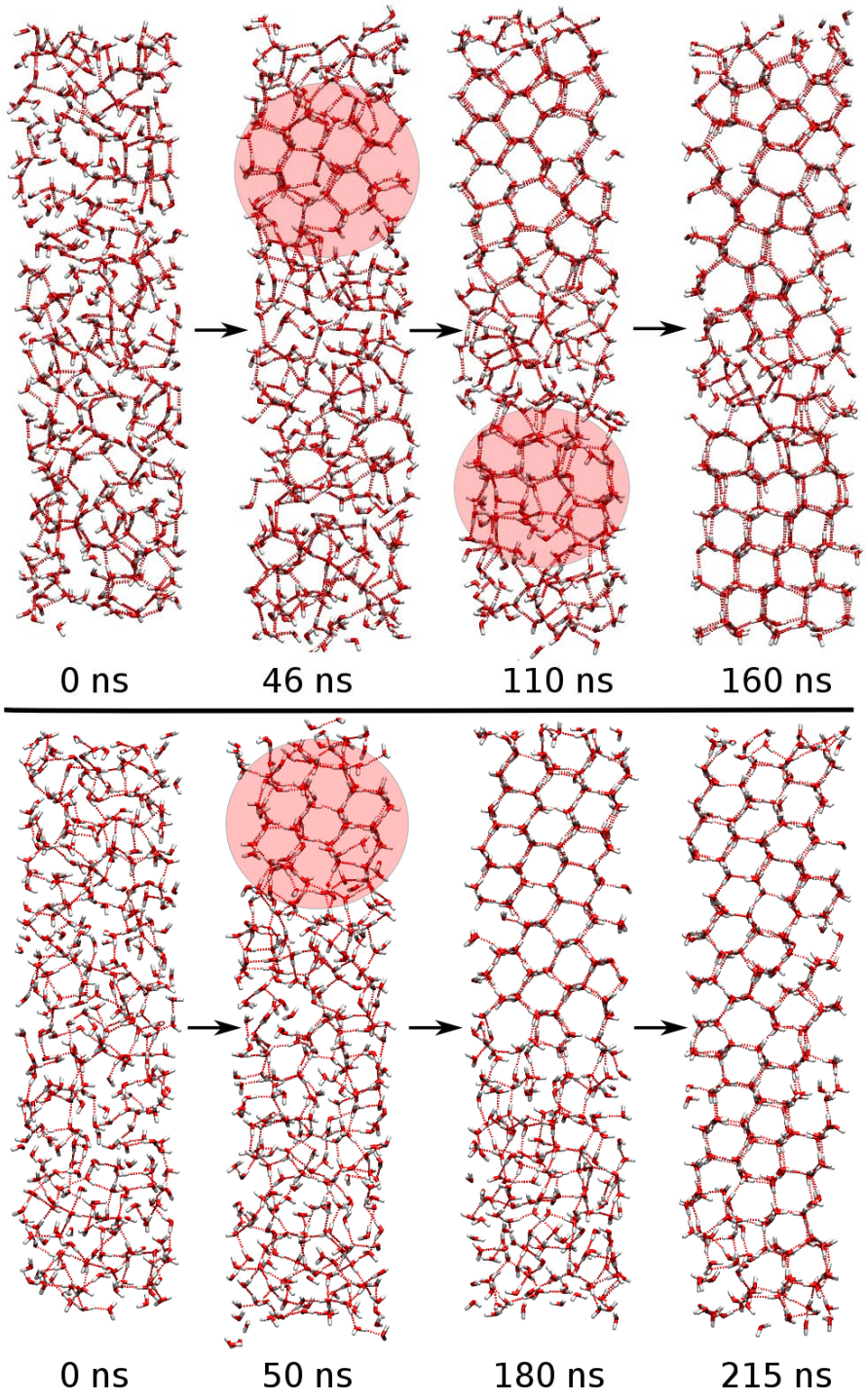

Fig. 2 (Vrbka & Jungwirth)

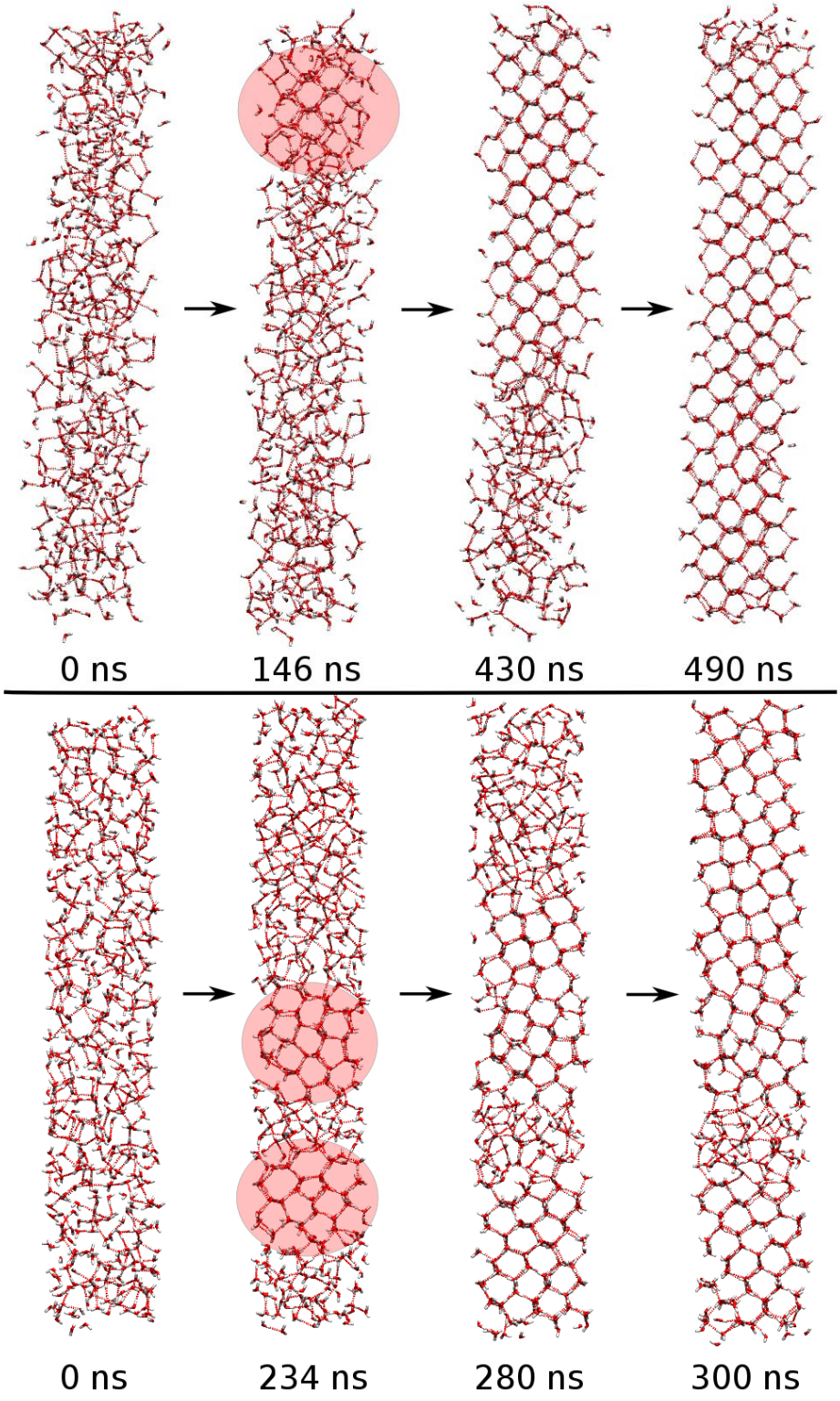

Fig. 3 (Vrbka & Jungwirth)

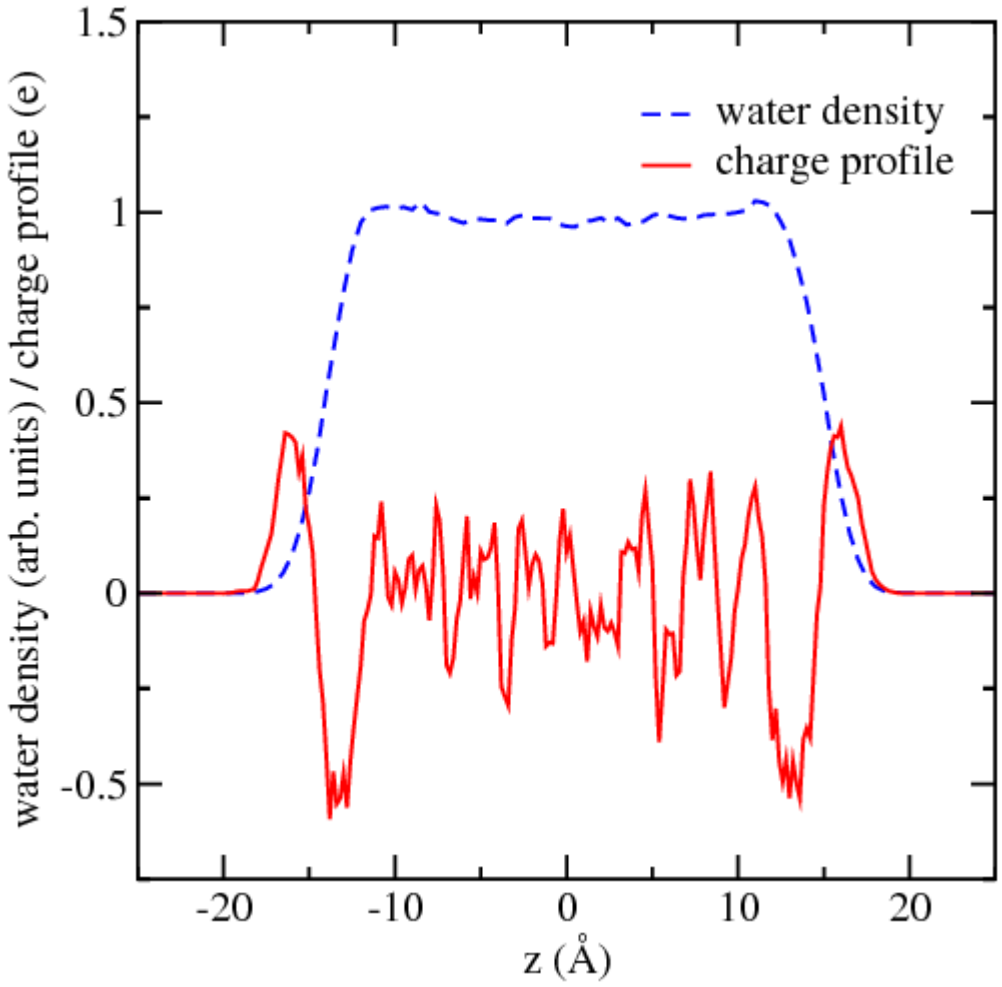

TOC (Vrbka & Jungwirth)